Available online at www.elixirpublishers.com (Elixir International Journal)

Nonlinear Dynamics

Elixir Nonlinear Dynamics 97 (2016) 42066-42069

ISSN: 2229-712X

Hyperchaotic Behaviour of a Fourth-Order Autonomous Electric Circuit with a Diode Pair

S. Manimaran[1], V. Balachandran[2,*] and G. Kandiban[3]

[1]Department of Physics, Roever Engineering College, Perambalur 621 212, India.

[2]Department of Physics, A.A. Govt. Arts College, Musiri Tiruchirappalli 621 211, India.

[3]Department of Physics, Vivekanandha College of Arts and Sciences for Women, Tiruchengode 637 205, India.

ARTICLE INFO

Article history:

Received: 9 July 2016;

Received in revised form:

30 July 2016;

Accepted: 5 August 2016;

Keywords

Fourth-order autonomous electric circuit,

smooth cubic nonlinearity,

chaos,

hyperchaos.

ABSTRACT

In this paper, in order to show some interesting phenomena of fourth-order hyperchaotic autonomous electric circuit with a smooth cubic nonlinearity, different kinds of attractors, time waveforms and corresponding power spectra of systems are presented, respectively. The perturbation transforms an unpredictable hyperchaotic behavior into a predictable hyperchaotic or periodic motion via stabilization of unstable, aperiodic, or periodic orbits of the strange hyperchaotic attractor. One advantage of the method is its robustness against noise. A theoretical analysis of the circuit equations is presented, along with experimental simulation and numerical results.

1.Introduction

In original Chua's circuit, a nonlinear resistor is called Chua's diode is the unique nonlinear electric element. It plays an important role in the circuit. Due to the existence of this nonlinear element Chua's circuit exhibits a variety of nonlinear phenomena, such as chaos, bifurcation and so on [1-5]. The characteristic of Chua's diode is described by a continuous piecewise - linear function with three segments and two no differential break points [6-9]. However, the characteristics of nonlinear devices in practical circuits are always smooth and the implementation of piecewise-linear function requires a large amount of circuitry compared with smooth cubic function. Therefore, it is significant to investigate Chua's circuit with a smooth cubic nonlinearity from practical view point [17]. Hartley (1989) proposed to replace the piecewise-linear nonlinearity in Chua's circuit with a smooth cubic nonlinearity.

In the present report the behavior of a hyperchaotic fourth-order autonomous electric circuit has been studied. This circuit consists of two active elements, one linear negative conductance and one smooth cubic nonlinearity exhibiting a symmetrical piecewise-linear *v-i* characteristic. Two inductances (L_1, L_2), two capacitances (C_1, C_2) and the capacitance C_2 serve as the control parameter.

Hyperchaos is defined as a chaotic attractor with more than one positive Lyapunov exponents, i.e., its dynamics expand in more than one direction [5]. In otherwords, the dynamics expand not only small line segments, but also small area elements, there giving rise to a 'thick' chaotic attractor. Most hyperchaotic and bifurcation effects cited in the literature have been observed in electric circuits. They include the period-doubling route to chaos, the intermittency route to chaos, and the quasiperiodicity route to chaos and of course the crisis [7-12]. This popularity is attributed to the advantages which electric circuits offer to experimental hyperchaos studies, such complicated hyperchaotic wave forms are expected to be utilized for realization of several hyperchaotic applications such a chaos communication system with robustness against various interferences including multi-user access [9-17]. The plan of the paper is as follows. In section 2, we present the details of realization of the proposed autonomous circuit. The results of the observations from the laboratory experimental simulation and the conformation through analytical calculation and numerical simulation on the dynamics of the circuit are presented in section 3. Finally, in section 4, we summarize and conclude the results and indicate further direction.

2. Circuit description and Simulation results

The fourth-order hyperchaotic autonomous electric circuit we have studied is presented in Fig. 1. It consists of two active elements, one linear negative conductance (G_1) and smooth cubic nonlinearity with an odd symmetric piecewise-linear *v-i* characteristic [17]. This fourth-order circuit is based on a third-order autonomous piecewise-linear circuit introduced by Chua and Lin, capable to realize every member of the Chua's circuit family [9]. Applying Kirchoff's laws, the set of four first-order coupled autonomous differential equations as given below:

$$C_1 \frac{dV_1}{dt} = -i_N - i_{L_1} \tag{1}$$

$$C_2 \frac{dV_2}{dt} = i_N - i_{L_2}$$

$$L_1 \frac{di_{L_1}}{dt} = \frac{i_{L_1}}{G_1} - V_1$$

$$L_2 \frac{di_{L_2}}{dt} = V_2$$

Tele:

E-mail address: brsbala@rediffmail.com

While V_1 and V_2 are the voltages across the Capacitors C_1 and C_2, i_{L1} and i_{L2} denotes the currents through the inductances L_1 and L_2 respectively and the characteristics of linear negative conductance is mathematically represented by $i_{G1} = - G_1 V_1$. Here the term $i_N = f(V_1-V_2)$ representing the characteristic of the smooth cubic nonlinearity can be expressed mathematically:

$$f(V_1-V_2) = a(V_1-V_2)+b(V_1-V_2)^3 \quad (2)$$

For our present experimental study we have chosen the following typical values of the circuit in Fig. 1. Were L_1 = 85 *mH*, L_2 = 33 *mH*, C_1 = 10 *nF*, C_2 = 33 *nF* and the characteristics of linear negative conductance G_1 = -0.5 *mS*. Here the variable capacitor 'C_2' is assumed to be the control parameter. By increasing the value of 'C_2' from 5 *nF* to 33 *nF*, the circuit behavior of Fig. 1 is found to transit from a period-doubling route to chaos and then to hyperchaotic attractor through period-doubling bifurcation behavior followed by period-doubling windows and boundary crisis [13-16], etc. The hyperchaotic attractors of fourth-order autonomous circuit with the smooth cubic nonlinearity projected onto different planes are shown in Fig. 2. Experimental time series were registered using a simulation storage oscilloscope for discrete values of C_1 and C_2 are shown if Fig. 3.

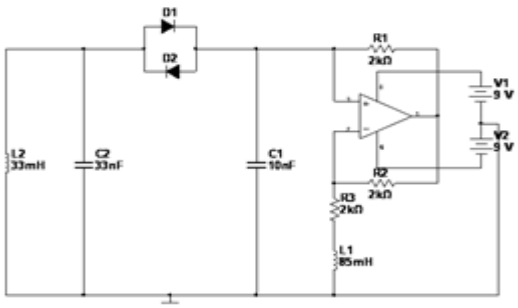

Fig 1. Circuit realization of the fourth-order hyperchaotic autonomous electric circuit.

The distribution of power in a signal *x(t)* is the most commonly quantified by means of the power density spectrum or simply power spectrum. It is the magnitude-square of the Fourier transforms of the signal *x(t)*. It can detect the presence of hyperchaos when the spectrum is broad-banded. The power spectrum corresponding to the voltages $V_1(t)$ and $V_2(t)$ waveforms across the capacitors C_1 and C_2 for the hyperchaotic regimes are shown in Fig. 4 which resembles broad-band spectrum noise.

3. Numerical confirmation

The hyperchaotic dynamics of circuit as shown in Fig. 1 is studied by numerical integration of the normalized differential equations [14]. For a convenient numerical analysis of the experimental system given by Eq. (1), we rescale the parameters as

$$V_1 = V x_1, V_2 = V x_2, i_{L_1}$$

$$= \sqrt{\frac{C_1}{L_1}} V x_3, i_{L_2} = \sqrt{\frac{C_1}{L_1}} V x_4, \alpha_1$$

$$= a\sqrt{\frac{L_1}{C_1}}, \alpha_2 = b\sqrt{\frac{L_1}{C_1}}, \upsilon = \frac{C_1}{C_2}, \gamma$$

$$= \frac{1}{G_1}\sqrt{\frac{C_1}{L_1}}, \beta = \frac{L_1}{L_2},$$

and then redefine τ as t. Eqs. (1) and (2) reduce to the following set of normalized equations of the fourth-order hyperchaotic autonomous electric circuit as given below:

$$\dot{x}_1 = -(\alpha_1(x_1-x_2)+\alpha_2(x_1-x_2)^3+x_3) \quad (3)$$

$$\dot{x}_2 = \upsilon(\alpha_1(x_1-x_2)+\alpha_2(x_1-x_2)^3-x_4)$$

$$\dot{x}_3 = \gamma x_3 - x_1$$

$$\dot{x}_4 = \beta x_2$$

The dynamics of Eq. (3) now depends upon the parameters α_1, α_2, υ, γ, and β. The experimental results have been verified by numerical simulation of the normalized Eq. (3) using the standard fourth-order Runge-Kutta method for a specific choice of system parameters employed in the experimental simulation results. That is, in the actual experimental set up the capacitor 'C_2' is varied from C_2 = 5 *nF* upward to 33 *nF*. Therefore in the numerical simulation, we study the corresponding Eq. (3) for in the range C_2 = 5 *nF* to 33 *nF*. From our numerical investigations, we find that for the value of 'C_2' above 5 *nF* periodic limit cycle motions is obtained. When the value of 'C_2' is increased to higher than 33 *nF* particularly in the range C_2 = (5 *nF* to 33 *nF*) the system displays a period-doubling route to chaos and then to

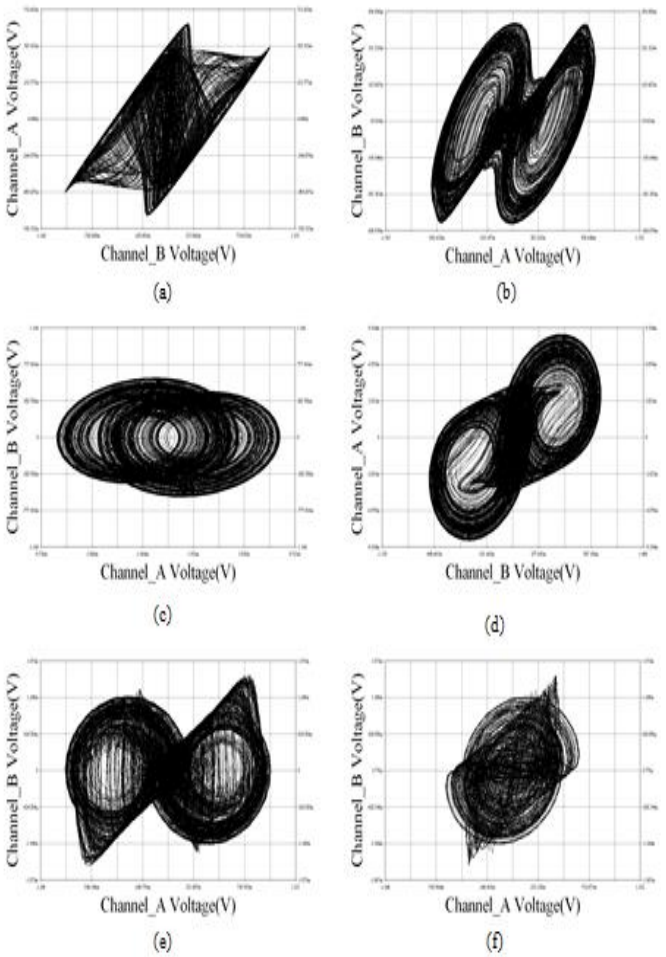

Fig 2. Simulation results of the projections of hyperchaotic attractor onto different planes.

hyperchaos through boundary condition [8]. These numerical results of the hyperchaotic attractor of fourth-order autonomous circuit with the smooth cubic nonlinearity projected onto different planes are shown in Fig. 5.

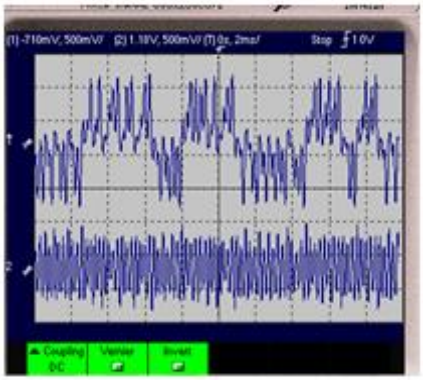

Fig 3. Simulation results of the hyperchaotic time series.

Fig. 6. shows the numerical chaotic time series was registered using a discrete value of 'C_2' serving as the control parameter. It is gratifying to note that the numerical results agree qualitatively very well with that of the experimental simulation results.

3.1 One parameter bifurcation diagram and Lyapunov exponents

The main features of the fourth-order hyperchaotic autonomous electric circuit can be summarized in the one parameter bifurcation diagram drawn in the (C_2 − x_2) plane (Fig. 7 (a)). Note that x_2 is the rescaled variable in Eqns. (3), $x_2 = V_2/V$. This bifurcation diagram clearly indicates that in the region C_2 = (5 nF, 30 nF) the system undergoes period-doubling bifurcation sequence to chaos, shows periodic windows through hyperchaotic region are observed in Fig. 1.

The Lyapunov exponent's λ_1, λ_2, λ_3 and λ_4 were obtained using the Wolf algorithm. For periodic orbits $\lambda_1 = 0$, λ_2, λ_3, $\lambda_4 < 0$, for quasi-periodic orbits $\lambda_1 = \lambda_2 = 0$, λ_3, $\lambda_4 < 0$, while for chaotic attractor $\lambda_1 > 0$, $\lambda_2 = 0$, λ_3, $\lambda_4 < 0$ and for hyperchaotic attractor $\lambda_1 > \lambda_2 > 0$, $\lambda_3 = 0$, $\lambda_4 < 0$. The Lyapunov spectrum in the (C_2 − λ_1, λ_2) plane, that is the first two maximal Lyapunov exponents versus fixed range of the control parameter as C_2 is increased, is shown in Fig. 7 (b). This correlates to the bifurcation diagram, Fig 7 (a). In the range (30 nF > C_2 > 5 nF) the system exhibits periodic windows with no positive Lyapunov exponent. When C_2 is increased further in the range (30 nF > C_2 > 5 nF), the system becomes chaotic with a single positive Lyapunov exponent (λ_1).

The chaotic nature is also characterized by a single positive Lyapunov exponent (λ_1). It is quite fascinating to look at the window region in the range (30 nF > C_2 > 5 nF), which corresponds to an entirely different dynamical behavior. It has been observed that for C_2 > 5 nF the attractors of the system are in any one of the smooth regions of the piecewise segments. Correspondingly, the attractors exhibit one of the generic types of bifurcations, namely period-doubling, saddle-node, or hopf-bifurcations. A section of the bifurcation diagram and the Lyapunov spectrum for the range 30 nF > C_2 > 5 nF are shown in Figs. 7 (a) and 7 (b), respectively, for clarity. The Lyapunov spectrum in the (C_2−λ_1, λ_2) plane, that is the first two maximal Lyapunov exponents versus fixed range of the control parameter as C_2 is increased, the hyper chaotic Lyapunov exponents shown in Fig. 7 (b) for C_2 = 20.05 nF the Lyapunov exponents are λ_1 = 0.14291, λ_2 = 0.00025, λ_3 = −0.78426 and λ_4 = −9.55430.

4. Conclusions

We have presented a fourth-order hyperchaotic autonomous electric

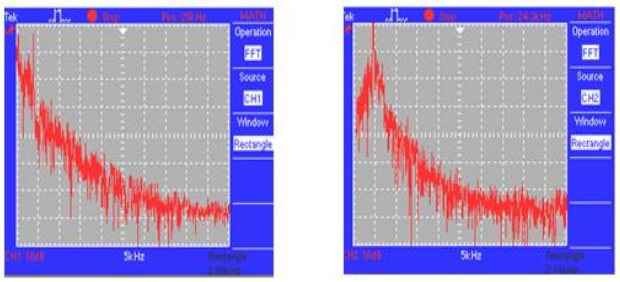

(a) (b)

Fig 4. Simulation results of the projections of hyperchaotic power spectrum.

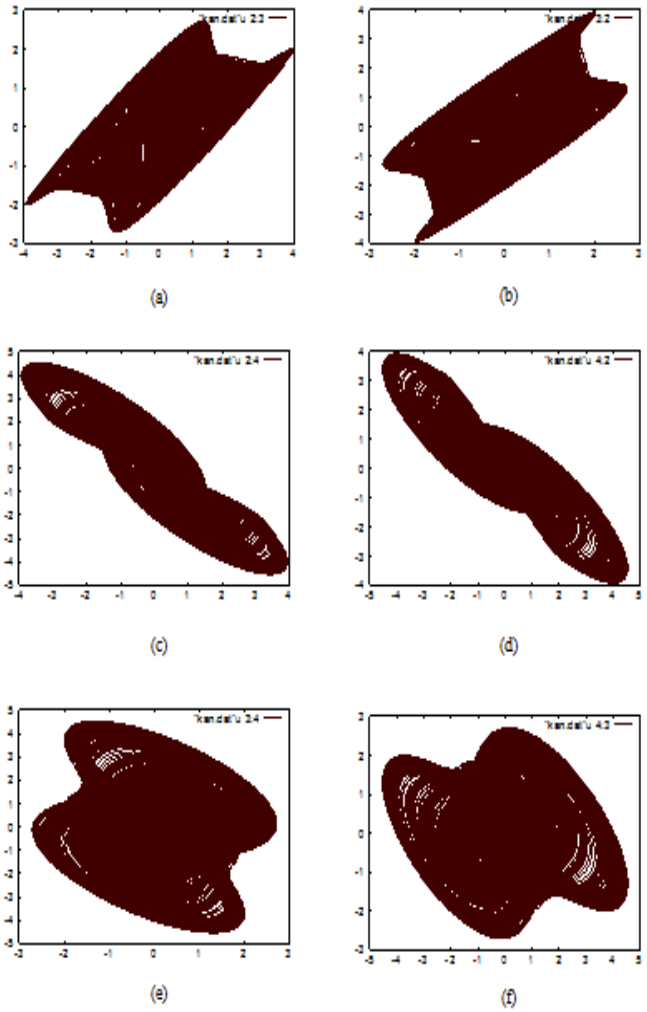

(a) (b) (c) (d) (e) (f)

Fig 5. Numerical results of the projections of hyperchaotic attractor onto different planes.

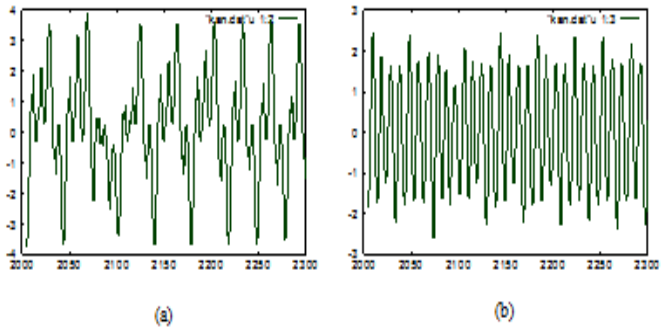

(a) (b)

Fig 6. Numerical results of the hyperchaotic time series.

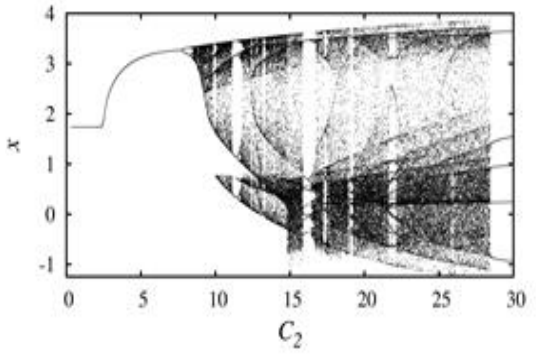

Fig 7a. For the normalized Eq. (3): One parameter bifurcation diagram in the ($C_2 - x_2$) plane at fixed range of control parameter of C_2 = (5 nF, 30 nF).

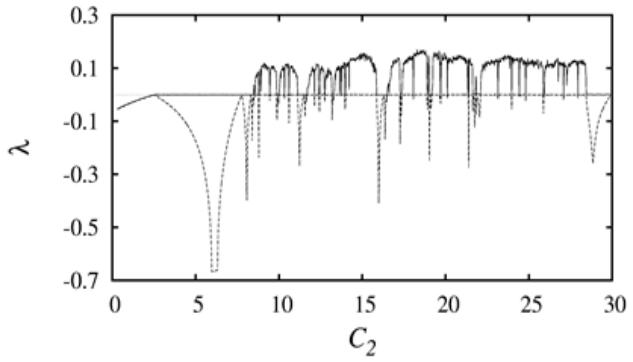

Fig7b. For the normalized Eq. (3): Two largest Lyapunov exponents versus C_2 for two trajectories in the ($C_2 - \lambda 1, \lambda 2$) plane.

Circuit which has symmetrical piecewise-linear elements. We can confirm hyperchaotic attractor on computer simulation or circuit experiments. The attractive feature of this circuit is the presence of hyperchaotic attractor over a range of parameter values, which might be useful for applications in controlling of hyperchaos, synchronization and in secure communication system.

References

[1] I M Kyprianidis, I N Stouboulos, P Haralabidis and T Bountis, *Int. J. Bifurc. and Chaos.* 8, 1903 (2000)
[2] L O Chua and G N Lin, *IEEE Trans. Circ. Syst*.CAS-38, 510 (1991)
[3] M P Kennedy, *IEEE Trans. Circ. Syst. I*. 40, 640 (1993)
[4] K Murali and M Lakshmanan, *Int. J. Bifurc. and Chaos*. 1, 369 (1991)
[5] T Motsumoto, L O Chua and K Kobaiashi, *IEEE Trans. Circ. Syst*. CAS-33, 1143 (1986)
[6] A Tamasevicius, A Namajunas and A Cenys, *Electron. Lett*. 32, 957 (1996)
[7] K Thamilmaran, M Lakshmanan and A Venkatesan, *Int. J. Bifurc. and Chaos*. 14, 221 (2004)
[8] R Barboza, *Int. J. Bifurc. and Chaos.* 18, 1151 (2008)
[9] L O Chua and G N Lin, *IEEE Trans. Circ. Syst.* 37, 885 (1990)
[10] V Balachandran and G Kandiban, *Indian J. Pure and Appl. Phys.* 47, 823 (2009)
[11] A Tamasevicius, A Cenys, G Mykolaitis, A Namajunas and E Lindberg, *Electron. Lett.* 33, 542 (1997)
[12] A Tamasevicius and A Cenys, *Chaos, Solit. and Fract*. 9, 115 (1998)
[13] C L Koliopanos, I M Kyprianidis, I N Stouboulos, A N Anagnostopoulos and L Magafas, *Chaos, Solit. and Fract.* 16,173 (2003)
[14] X Liu, J Wang and L Huang, *Int. J. Bifurc. and Chaos.* 17, 2705 (2007)
[15] R Barboza and L O Chua, *Int. J. Bifurc. and Chaos.* 18, 943 (2008)
[16] T Kapitaniak and L O Chua, *Int. J. Bifurc. and Chaos.* 4, 477 (1994)
[17] G P King and S T Gaito, *Phys. Rev. A.* 46, 3093 (1992).